AJNR

Pseudo-Resting-State Functional MRI Derived from Dynamic Susceptibility Contrast Perfusion MRI Can Predict Cognitive Impairment in Glioma

Nicholas S. Cho, Chencai Wang, Kathleen Van Dyk, Francesco Sanvito, Sonoko Oshima, Jingwen Yao, Albert Lai, Noriko Salamon, Timothy F. Cloughesy, Phioanh L. Nghiemphu and Benjamin M. Ellingson

Pseudo-Resting-State Functional MRI Derived from Dynamic Susceptibility Contrast Perfusion MRI Can Predict Cognitive Impairment in Glioma

Nicholas S. Cho, Chencai Wang, Kathleen Van Dyk, Francesco Sanvito, Sonoko Oshima, Jingwen Yao, Albert Lai, Noriko Salamon, Timothy F. Cloughesy, Phioanh L. Nghiemphu, and Benjamin M. Ellingson

ABSTRACT

BACKGROUND AND PURPOSE: Resting-state functional MRI (rs-fMRI) can be used to estimate functional connectivity (FC) between different brain regions, which may be of value for identifying cognitive impairment in patients with brain tumors. Unfortunately, neither rs-fMRI nor neurocognitive assessments are routinely assessed clinically, mostly due to limitations in examination time and cost. Since DSC perfusion MRI is often used clinically to assess tumor vascularity and similarly uses a gradient-echo-EPI sequence for T2*-sensitivity, we theorized a "pseudo-rs-fMRI" signal could be derived from DSC perfusion to simultaneously quantify FC and perfusion metrics, and these metrics can be used to estimate cognitive impairment in patients with brain tumors.

MATERIALS AND METHODS: Twenty-four consecutive patients with gliomas were enrolled in a prospective study that included DSC perfusion MRI, resting-sate functional MRI (rs-fMRI), and neurocognitive assessment. Voxelwise modeling of contrast bolus dynamics during DSC acquisition was performed and then subtracted from the original signal to generate a residual "pseudo-rs-fMRI" signal. Following the preprocessing of pseudo-rs-fMRI, full rs-fMRI, and a truncated version of the full rs-fMRI (first 100 timepoints) data, the default mode, motor, and language network maps were generated with atlas-based ROIs, Dice scores were calculated for the resting-state network maps from pseudo-rs-fMRI and truncated rs-fMRI using the full rs-fMRI maps as reference. Seed-to-voxel and ROI-to-ROI analyses were performed to assess FC differences between cognitively impaired and nonimpaired patients.

RESULTS: Dice scores for the group-level and patient-level (mean±SD) default mode, motor, and language network maps using pseudo-rs-fMRI were 0.905/0.689 ± 0.118 (group/patient), 0.973/0.730 ± 0.124, and 0.935/0.665 ± 0.142, respectively. There was no significant difference in Dice scores between pseudo-rs-fMRI and the truncated rs-fMRI default mode ($P = .97$) or language networks ($P = .30$), but there was a difference in motor networks ($P = .02$). A multiple logistic regression classifier applied to ROI-to-ROI FC networks using pseudo-rs-fMRI could identify cognitively impaired patients (sensitivity = 84.6%, specificity = 63.6%, receiver operating characteristic area under the curve (AUC) = 0.7762 ± 0.0954 (standard error), $P = .0221$) and performance was not significantly different from full rs-fMRI predictions (AUC = 0.8881 ± 0.0733 (standard error), $P = .0013$, $P = .29$ compared with pseudo-rs-fMRI).

CONCLUSIONS: DSC perfusion MRI-derived pseudo-rs-fMRI data can be used to perform typical rs-fMRI FC analyses that may identify cognitive decline in patients with brain tumors while still simultaneously performing perfusion analyses.

ABBREVIATIONS: ASL = arterial spin-labeling; AUC = area under curve; BOLD = blood oxygenation level–dependent; FC = functional connectivity; FDR = false discovery rate; FWE = family-wise error; MNI = Montreal Neurological Institute; ROC = receiver operating characteristic; rs-fMRI = resting-state functional MRI

Although management of brain tumor patients typically involves assessing changes in tumor size on anatomic MRI techniques (e.g., T2-weighted FLAIR and contrast-enhanced T1-weighted images), the utilization of advanced MRI techniques is becoming more common and may provide valuable new insights into tumor biology and other important information that may improve clinical management. For example, evidence

SUMMARY SECTION

PREVIOUS LITERATURE: Resting-state network analyses from resting-state functional MRI (rs-fMRI) are of great interest in patient populations for potential clinical utility in presurgical mapping and for studying neurocognition. However, rs-fMRI and neuropsychological test batteries are not routinely performed clinically. We theorized that "pseudo-rs-fMRI" data can be derived from the more widely performed dynamic susceptibility contrast perfusion MRI because of this imaging technique's similar T2*-sensitivity as in rs-fMRI. We compared the performance of our proposed pseudo-rs-fMRI approach and rs-fMRI in generating resting-state network maps and predicting cognitive impairment status in patients with gliomas off-therapy.

KEY FINDINGS: Patient-level and group-average default mode, language, and motor network map Dice scores were similar between pseudo-rs-fMRI and rs-fMRI. Additionally, both pseudo-rs-fMRI and rs-fMRI functional connectivity results were able to predict cognitive impairment status in glioma patients ($P < .05$), and performance was not significantly different ($P > .05$).

KNOWLEDGE ADVANCEMENT: Our pseudo-rs-fMRI approach by using DSC perfusion MRI has significant clinical implication by enabling simultaneous perfusion and rs-fMRI analyses from a single DSC perfusion MRI acquisition. The presented method can be applied retrospectively or integrated prospectively into clinical workflows. Additionally, we propose a dually-optimized DSC perfusion MRI for both analyses.

suggests blood oxygenation level—dependent (BOLD) resting-state functional MRI (rs-fMRI)[1,2] may have clinical utility for presurgical mapping (e.g., motor and language networks).[3-7] Additionally, rs-fMRI measures of functional connectivity (FC)—particularly within the default mode network[8,9]—may be useful for studying neurocognition in patient populations, including patients with brain tumors.[10-14] Neurocognitive assessment in patients with brain tumors is particularly important for therapeutic response evaluation[15] and is gaining considerable attention because reduced neurocognition has a profound impact on posttreatment morbidity and cancer survivorship.[16]

Unfortunately, neither rs-fMRI nor neuropsychological test batteries are routinely performed clinically, mostly due to limitations in examination time and cost. As a result, there is a present need to be able to conduct rs-fMRI analyses and to identify cognitive decline in patients within current clinical workflows. Of note, during a rs-fMRI scan, patients are scanned using a T2*-sensitive sequence while at "rest,"[1] precluding the need for task paradigms. Based on MR physics principles, it may be conceivable to acquire "pseudo-rs-fMRI" data from a DSC perfusion MRI scan. DSC perfusion MRI is also dynamically-acquired with a T2*-sensitive gradient-echo-EPI sequence with strong BOLD-weighting like BOLD rs-fMRI, except DSC is performed during the injection of a contrast agent bolus. DSC perfusion MRI is also used much more extensively in clinical settings than BOLD rs-fMRI for brain tumors to assess tumor vascularity.[17-20]

We theorized a "pseudo-rs-fMRI" signal could be derived from DSC perfusion to quantify FC and that these metrics can be used to estimate cognitive impairment in patients with brain tumors. We hypothesized that: (1) pseudo-rs-fMRI derived from

DSC perfusion MRI would yield similar qualitative network mapping results as rs-fMRI by investigating 3 commonly studied resting-state networks given their relevance to clinical care and neuroscience research: the default mode, motor, and language networks;[8,9,21] and (2) there would be observable FC differences between cognitively impaired-versus-nonimpaired patients, particularly of the default mode network, using rs-fMRI and pseudo-rs-fMRI.

MATERIALS AND METHODS

Study Design

This study was performed in compliance with the Health Insurance Portability and Accountability Act (HIPAA) and was approved by our institutional review board. All patients provided informed consent. Consecutive patients seen at our neuro-oncology clinic that were previously diagnosed with diffuse glioma and had completed all therapies/surgeries and were off-therapy for at least 6 months before enrollment in a prospective trial (IRB #17–001500) assessing cognitive assessment using a neuropsychological test battery were eligible for study.[14] The inclusion criteria for the present study were: (1) right-handed, (2) received rs-fMRI scanning, and (3) received DSC perfusion MRI with near whole-brain coverage within the same session. A total of 24 consecutive patients with the above inclusion criteria were recruited. Clinical data are summarized in Table 1 with further detailed diagnosis provided in the Online Supplemental Data. A portion of patients were assessed in a prior study.[14]

Cognitive Impairment Assessment

Cognitive function was assessed using a previously described neuropsychological test battery[14] informed by International Cognition and Cancer Task Force recommendations,[22] expert recommendations,[23] and the authors' prior clinical experience. The test battery included learning, memory, attention, processing speed, working memory, language, and visuospatial measures (see the Online Supplemental Data for a detailed assessment list).[14] Each score was normalized to Z-scores using published normative data as a reference. Patients were categorized as "cognitively impaired" if 2 or

Please address correspondence to Benjamin M. Ellingson, PhD, Director, UCLA Brain Tumor Imaging Laboratory (BTIL), Professor of Radiology, Psychiatry, and Neurosurgery, Departments of Radiological Sciences, Psychiatry, and Neurosurgery, David Geffen School of Medicine, University of California, Los Angeles, 924 Westwood Blvd, Suite 615, Los Angeles, CA 90024; e-mail: bellingson@mednet.ucla.edu; Phone: 310-481-7572, Fax: 310-794-2796

Table 1: Patient data

Characteristic	No.
Age (yr)	
Average	45
Range	22–70
Sex	
Male	16
Female	8
Cognitive impairment status	
Impaired	13
Nonimpaired	11
Handedness	
Right	24
Left	0
IDH Status	
Mutant	19
Wild-type	2
Unknown	3

Table 2: DSC perfusion MRI and full resting-state functional MRI parameters

	Patient Cohort (*N* = 24)	
Sequence	Full Rs-fMRI	DSC Perfusion
No. of patients	24	24
Scanner model	Prisma, Skyra, Vida	
Field strength	3T	3T
TE	28 ms	17 ms
TR	2 sec	1.35–1.72 sec
Flip angle	77°	35°
No. of volumes	300 (265 for *n* = 1)	120
No. of slices	38	24–30
Slice thickness	4 mm	5 mm
Acquisition matrix	64 × 64	128 × 128
Field of view	220 mm	240 mm

more of their test scores were $Z \leq -2$ and as "cognitively nonimpaired" if otherwise; criteria were based on the International Cognition and Cancer Task Force recommendations and accounting for the number of tests to limit the likelihood of falsely identifying chance impairment.[22,24]

Image Acquisition

MPRAGE T1 pre-/postcontrast MRI, T2-weighted FLAIR MRI, DSC perfusion MRI, and rs-fMRI scans were acquired at 3T using Prisma, Magnetom Skyra, or Vida scanners (Siemens). Rs-fMRI was acquired during the same session as the anatomical and DSC perfusion MRI and before the DSC perfusion MRI as per recommended guidelines.[21] Anatomical MPRAGE T1 pre-/postcontrast MRI and T2-weighted FLAIR MRI were acquired in compliance with the standardized brain tumor imaging protocol.[25] All DSC perfusion MRI was acquired after administration of a 0.1-mmol/kg bolus of Gd-DTPA. Rs-fMRI and DSC perfusion MRI scan parameters are summarized in Table 2.

Image Preprocessing: Full and Truncated Resting-State Functional MRI

Full rs-fMRI data were preprocessed in accordance with recently published preprocessing recommendations[21] using the CONN toolbox (https://web.conn-toolbox.org/).[26] In brief, the standard CONN preprocessing pipeline steps of functional realignment/unwarping and slice-timing correction were performed. Next, outlier identification, image registration to the Montreal Neurological Institute space (MNI), and segmentation of gray matter, white matter, and CSF were performed. Then, the full rs-fMRI data were smoothed using an 8- mm full width at half maximum Gaussian kernel and denoised by regressing motion-correction parameters along with white matter and CSF signal and applying a bandpass filter of 0.01–0.1 Hz. Because DSC perfusion MRI is of shorter duration than typical rs-fMRI acquisitions, a truncated rs-fMRI was created by taking the first 100 volumes and preprocessing as described above to serve as a comparison.

Image Preprocessing: Pseudo-Resting-State Functional MRI from DSC Perfusion MRI

DSC perfusion MRI was preprocessed by first performing motion-correction using FSL's MCFLIRT function (https://fsl.fmrib.ox.ac.uk/fsl/fslwiki/MCFLIRT)[27] and then applying a bidirectional leakage-correction algorithm to obtain a leakage-corrected signal.[28-30] Pseudo-rs-fMRI data were then extracted by performing voxelwise, Gamma-variate modeling of the contrast agent bolus and then performing voxelwise subtraction of the modelled contrast agent bolus from the leakage-corrected signal to create a residual "pseudo-rs-fMRI" signal (Fig 1). Pseudo-rs-fMRI data were then loaded into the CONN toolbox[26] for further standard rs-fMRI-related preprocessing as performed for the rs-fMRI data in this study except for volume censoring.

Image Postprocessing: Generating Pseudo-/Resting-State Seed-to-Voxel Network Maps

Default mode network, motor network, and language network seed-to-voxel maps were generated for each patient in pseudo-rs-fMRI, full rs-fMRI, and truncated rs-fMRI using consistent seed ROIs selected from CONN's built-in network ROI parcellations in MNI atlas space.[26] Specifically, the default mode network was generated by seeding the medial prefrontal cortex ROI, the motor network was generated by seeding the left lateral sensorimotor cortex ROI, and the language network was generated by seeding the left inferior frontal gyrus ROI. Group-level average network maps were then created through the Analysis of Functional NeuroImages (AFNI; https://afni.nimh.nih.gov/)[31] 3dttest++ command. Dice scores were used to evaluate the similarity between rs-fMRI and pseudo-rs-fMRI. Dice scores range from 0 to 1, where a Dice score of 0 is no overlap and a Dice score of 1 is perfect overlap. Dice scores were computed for each patient and the group-average seed-to-voxel maps between the resting-state network maps generated by (1) pseudo-rs-fMRI and full rs-fMRI as well as (2) truncated rs-fMRI and full rs-fMRI using Matlab (MathWorks). Network map Dice scores for each image pairing were calculated within the overlap of perfusion slice coverage and regions of full rs-fMRI activation with $r > 0.3$ for pseudo-rs-fMRI versus full rs-fMRI and truncated rs-fMRI versus full rs-fMRI assessments.

Functional Connectivity Differences Based on Cognitive Impairment Status

When performing quantitative analyses assessing connectivity differences between cognitively impaired and nonimpaired patients, voxels within any resection cavities were excluded from the analyses. Resection cavity masks were segmented using AFNI
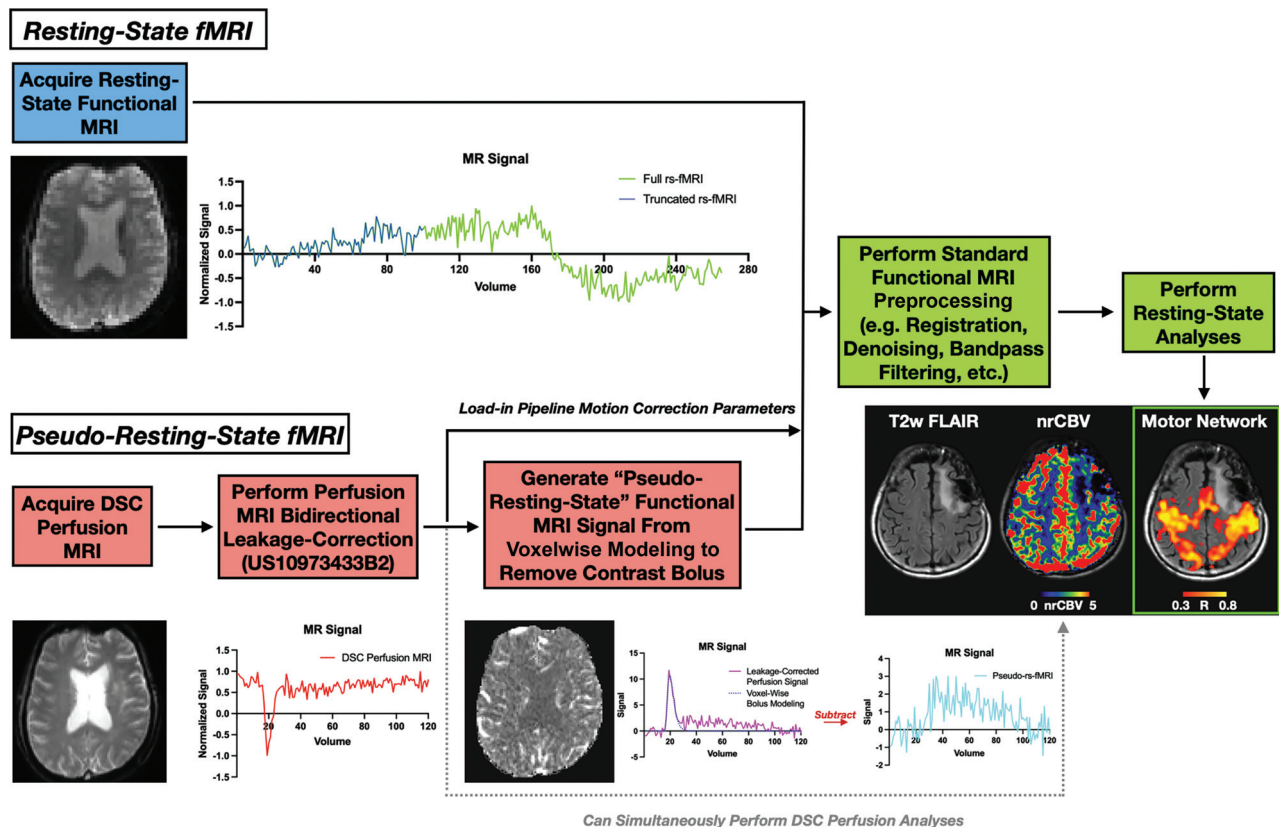
FIG 1. Schematic of pseudo- and resting-state functional MRI processing pipeline. Pseudo-resting-state functional MRI is derived from DSC perfusion MRI through bidirectional leakage-correction and voxelwise modeling of the contrast bolus and then incorporated into typical resting-state functional MRI preprocessing pipelines while still being able to simultaneously perform DSC perfusion MRI analyses. nrCBV indicates normalized relative CBV; T2W, T2WI.

software[31] and the MNI-registered T1-weighted precontrast or T2-weighted FLAIR MRI scans by a lab member with 2 years of tumor segmentation experience (N.S.C.) and inspected by a radiologist with 11 years of neuroimaging experience (S.O.), who were blinded to the cognitive impairment status.

Both seed-to-voxel and ROI-to-ROI approaches were performed to identify FC differences based on cognitive impairment status using pseudo-rs-fMRI and full rs-fMRI. For the seed-to-voxel approach, difference maps were generated using the AFNI *3dttest++* command. For the ROI-to-ROI approach, connectivity matrices were extracted for each individual patient using the CONN toolbox. To further account for prior surgical resection and larger rs-fMRI slice coverage compared with DSC perfusion MRI in some brain regions, the network ROIs were refined at the patient-level to exclude voxels outside the perfusion slice coverage and voxels within any prior resection cavities from quantitative FC analyses. ROIs in the cerebellum, supplementary motor area, and frontal eye fields were excluded from group analyses a priori due to limited perfusion slice coverage. Then, patient-specific ROIs were fed into CONN for signal extraction and further group difference analyses.

Statistical Analysis

Paired *t* tests or Wilcoxon signed-rank tests were performed at a threshold of $P < .05$ to compare Dice scores between pseudo-rs-fMRI and full rs-fMRI and truncated rs-fMRI and full rs-fMRI

network maps depending on the normality of the data. The potential relationship between tumor hemispheric lateralization and cognitive impairment status was assessed using the Fisher exact test. A multivariable general linear model was implemented to identify functional differences between cognitively impaired and nonimpaired patients for seed-to-voxel and ROI-to-ROI analyses using pseudo-rs-fMRI and full rs-fMRI with age and TR as covariates (see the Online Supplement Data for additional details). The level of significance for seed-to-voxel and ROI-to-ROI analyses for group differences was set at $P < .05$ with a false discovery rate (FDR) of 0.05. Multiple logistic regression was performed using ROI-to-ROI FC to predict cognitive impairment status using pseudo-rs-fMRI and full rs-fMRI, and paired analyses comparing the AUC of the resulting receiver-operating characteristic (ROC) curves was performed using the Hanley & McNeil's paired statistical method.[32]

RESULTS

Individual and Group-Level Functional Connectivity

Three representative patients and their default mode, motor, and language network map results using full rs-fMRI and pseudo-rs-fMRI are shown in Fig 2. Patient 1 is a 38-year-old male patient who is cognitively impaired and was diagnosed with *IDH*-mutant astrocytoma, and the Dice scores for the default mode, motor, and language networks were 0.873, 0.701, and 0.429, respectively (Fig 2A). Patient 2 is a 38-year-old male patient who is not
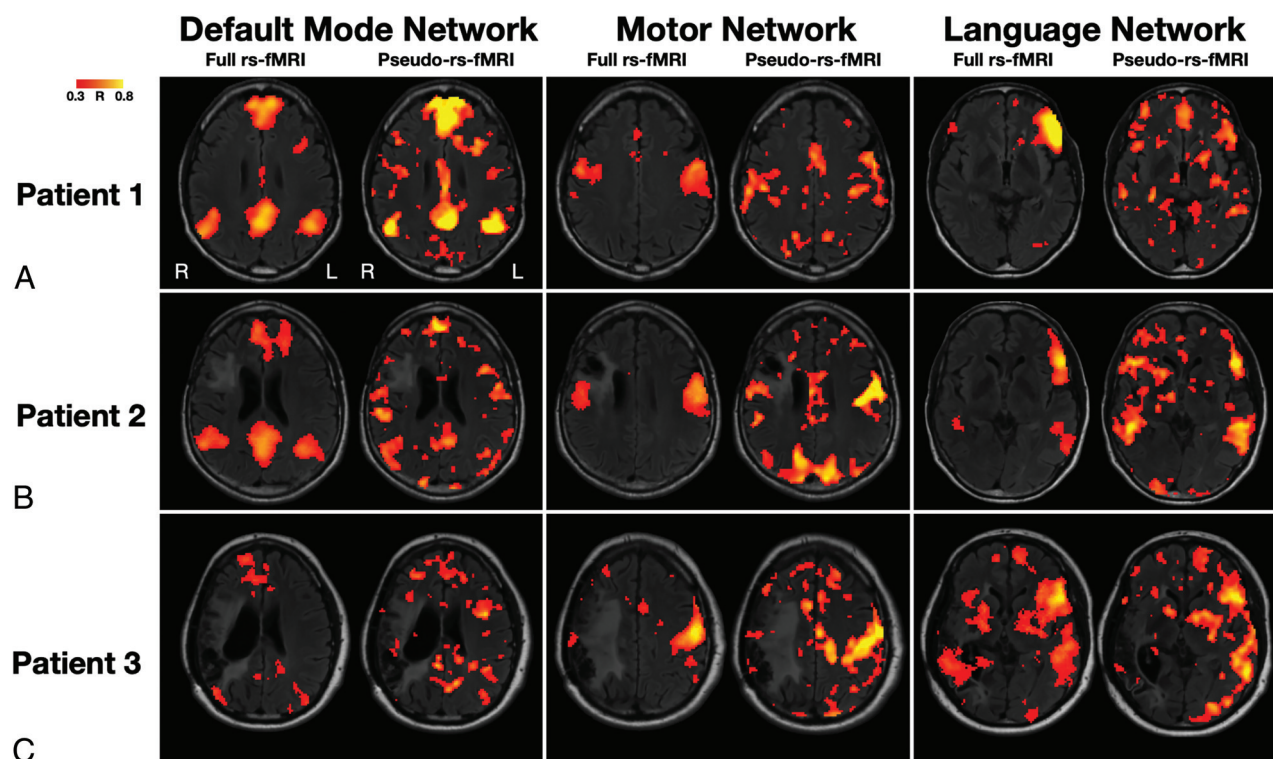
FIG 2. Three representative cases of default mode, motor, and language network maps using full rs-fMRI and pseudo-rs-fMRI. Patient 1 (*A*) is a 38-year-old male patient who is cognitively impaired and was diagnosed with *IDH*-mutant astrocytoma. Patient 2 (*B*) is a 38-year-old male patient who is not cognitively impaired and was diagnosed with *IDH*-mutant astrocytoma. Patient 3 (*C*) is a 41-year-old male patient who is not cognitively impaired and was diagnosed with *IDH*-mutant astrocytoma. See the Online Supplemental Data for network maps using truncated rs-fMRI. L indicates left; R, right.

cognitively impaired and was diagnosed with *IDH*-mutant astrocytoma, and the Dice scores for the default mode, motor, and language networks were 0.612, 0.740, and 0.819, respectively (Fig 2B). Patient 3 is a 41-year-old male patient who is not cognitively impaired and was diagnosed with *IDH*-mutant astrocytoma, and the Dice scores for the default mode, motor, and language networks were 0.472, 0.663, and 0.594, respectively (Fig 2C). The Online Supplemental Data show the network maps from pseudo-rs-fMRI and truncated rs-fMRI for comparison, the latter of which are visually noisier than those from the full rs-fMRI.

The mean and SD Dice scores between (1) pseudo-rs-fMRI and full rs-fMRI and (2) truncated rs-fMRI and full rs-fMRI are shown in Fig 3 and the Online Supplemental Data. The mean and SD Dice scores between pseudo-rs-fMRI and full rs-fMRI for the default mode, motor, and language networks were 0.689 (0.118), 0.730 (0.124), and 0.665 (0.142), respectively. There was no significant difference in Dice scores between pseudo-rs-fMRI and full rs-fMRI and truncated rs-fMRI and full rs-fMRI for the default mode network ($P = .97$, mean difference of pseudo-rs-fMRI minus truncated rs-fMRI Dice scores = 0.002, Fig 3A) or language network ($P = .30$, mean difference = 0.036, Fig 3C), but there was a significant increase in Dice scores for pseudo-rs-fMRI and full rs-fMRI compared with truncated rs-fMRI and full rs-fMRI for the motor network ($P = .02$, mean difference = 0.085, Fig 3B).

The averaged group maps of the default mode, motor, and language networks from full rs-fMRI and pseudo-rs-fMRI at

thresholds of $r > 0.2$ and $r > 0.3$, respectively, for visualization, are shown in Fig 4. The default mode network in pseudo-rs-fMRI and full rs-fMRI shows FC in the medial prefrontal cortex, left/right inferior parietal lobule, and posterior cingulate cortex. The motor network in pseudo-rs-fMRI and full rs-fMRI shows FC in the left and right sensorimotor cortex and the anterior cingulate cortex, although the anterior cingulate cortex is not visualized in the full rs-fMRI-derived motor network map at a higher, matched threshold of $r > 0.3$ (Online Supplemental Data). Similarly, the language network in pseudo-rs-fMRI and full rs-fMRI shows FC in the left and right inferior frontal gyrus and left Wernicke area, although the left Wernicke is not visualized in the full rs-fMRI-derived language network map at a higher, matched threshold of $r > 0.3$ (Online Supplemental Data). The Dice scores for the group maps are also presented in Fig 3 and the Online Supplemental Data, which ranged between 0.905 and 0.973 for pseudo-rs-fMRI and full rs-fMRI network maps.

Relationship between Functional Connectivity and Cognitive Impairment

Seed-to-voxel analyses did not show any significant cluster differences after family-wise error (FWE)-correction between cognitively impaired and nonimpaired patients when seeding the medial prefrontal cortex of the default mode network. Additionally, no significant differences were found in the results of seed-to-voxel analyses between full rs-fMRI and pseudo-rs-fMRI using an interaction model assessing for significant differences between the 2

techniques after FWE-correction. To further explore potential similarities between full rs-fMRI and pseudo-rs-fMRI results, the cluster threshold for full rs-fMRI was empirically chosen to select for the top ~5% largest clusters, which corresponded to a threshold of 300 mm^3. At this lowered threshold, full rs-fMRI revealed some significant functional differences between cognitively impaired and nonimpaired patients (voxels $P < .05$) that were also observed using pseudo-rs-fMRI with the same cluster threshold (voxels $P < .05$) (Online Supplemental Data). Upon seeding the medial prefrontal cortex of the default mode network, both full rs-fMRI and pseudo-rs-fMRI identified weaker connectivity to clusters in the bilateral precuneus in cognitively nonimpaired patients compared with the cognitively impaired patients (left precuneus: $P = .0050$ for full rs-fMRI, $P = .0193$ for pseudo-rs-fMRI, right precuneus: $P = .0064$ for full rs-fMRI, $P = .0260$ for pseudo-rs-fMRI, Online Supplemental Data) as well as stronger connectivity to

clusters in the right rostral middle frontal cortex ($P = .0007$ for full rs-fMRI, $P = .0068$ for pseudo-rs-fMRI, Online Supplemental Data) and right superior frontal cortex ($P = .0002$ for full rs-fMRI, $P = .0121$ for pseudo-rs-fMRI, Online Supplemental Data).

Similarly, in ROI-to-ROI analyses, neither the full rs-fMRI nor pseudo-rs-fMRI yielded significant differences in FC after FDR-correction between cognitively impaired and nonimpaired patients. Nevertheless, some reproducible ROI-to-ROI connectivity patterns were observed in the FDR-uncorrected results that were in line with the FWE-uncorrected seed-to-voxel results (Online Supplemental Data). Specifically, there was stronger connectivity from the medial prefrontal cortex of the default mode network to the right rostral prefrontal cortex of the salience network in cognitively nonimpaired patients compared with the cognitively impaired patients ($P = .0013$ for full rs-fMRI, $P = .053$ for pseudo-rs-fMRI, Online Supplemental Data). Analogous findings to the left rostral prefrontal cortex were only observed in full rs-fMRI ($P = .0004$ for full rs-fMRI, $P = .58$ for pseudo-rs-fMRI, Online Supplemental Data) as in the seed-to-voxel analyses (Online Supplemental Data). Additionally, there were trends for weaker connectivity from the medial prefrontal cortex of the default mode network to the posterior cingulate cortex of the default mode network in cognitively nonimpaired patients compared with the cognitively impaired patients ($P = .18$ for full rs-fMRI, $P = .10$ for pseudo-rs-fMRI, Online Supplemental Data).

When combining these 3 individual ROI-to-ROI FC results into a multiple logistic regression to predict cognitive impairment status, both full rs-fMRI and pseudo-rs-fMRI classified impairment status with significant AUCs (full rs-fMRI: AUC = 0.8881;
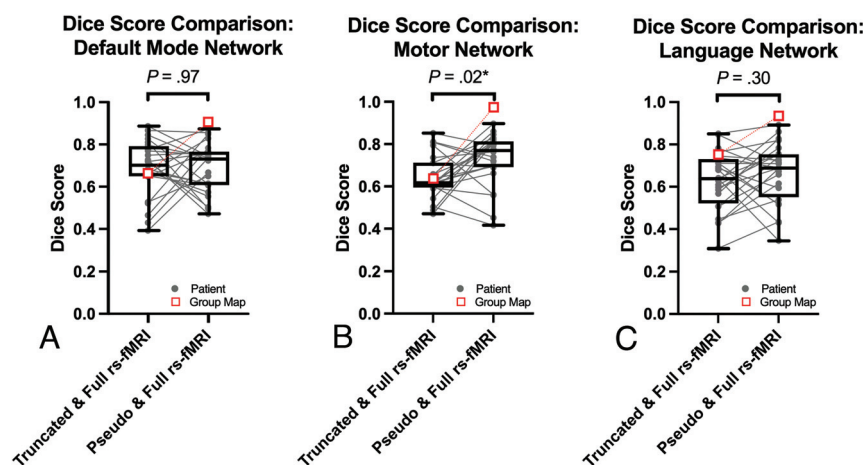
FIG 3. Comparison of Dice scores of network maps from pseudo-rs-fMRI and truncated rs-fMRI with full rs-fMRI. At the patient-level, no significant differences in Dice scores were observed for the default mode network (A) or language network (C), but there was a significant increase in Dice scores for pseudo-rs-fMRI compared with truncated rs-fMRI for the motor network (B). Boxplots of the patient-level data and singular Dice score values of the group-average maps (*red squares*) are also overlaid for visualization. The asterisk indicates statistical significance.

FIG 4. Group-average maps of default mode, motor, and language network maps using full rs-fMRI and pseudo-rs-fMRI. Network maps are presented using full pseudo-rs-fMRI (A) and pseudo-rs-fMRI (B). See the Online Supplemental Data for the network maps of full rs-fMRI at a matched $r > 0.3$ threshold. L indicates left; R, right.

Multiple Logistic Regression: Combining ROI-to-ROI Network FC to Predict Cognitive Impairment Status

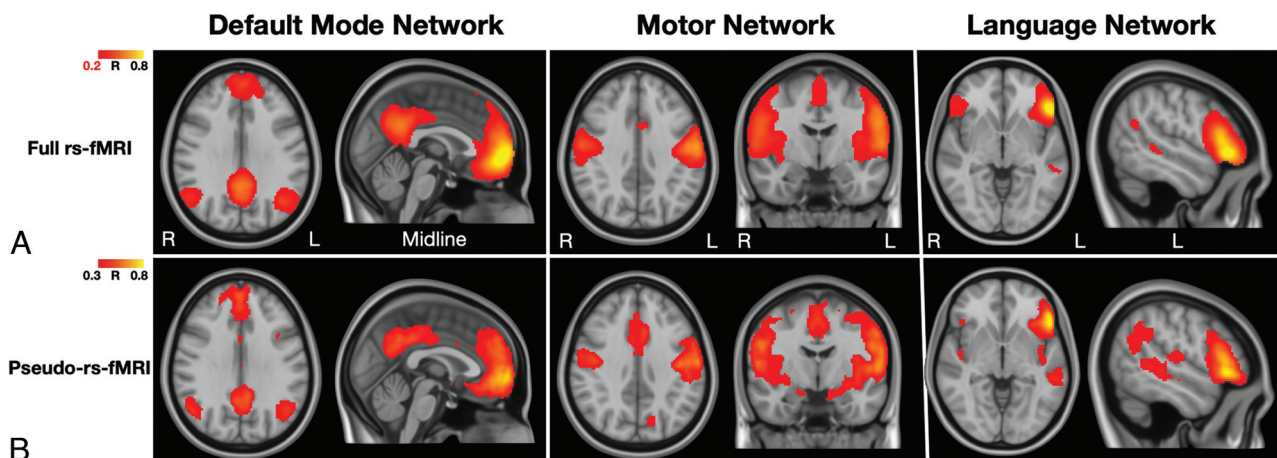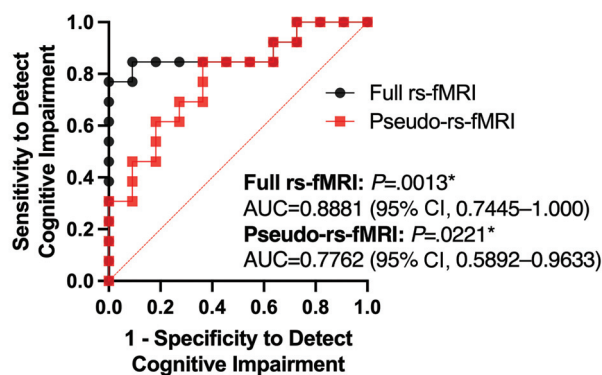**FIG 5.** Combining ROI-to-ROI connectivity alterations to predict cognitive impairment status. Multiple logistic regression ROC curve analyses combining ROI-to-ROI connectivity differences between cognitively impaired and nonimpaired patients demonstrated an AUC of 0.8881 ($P = .0013$) using full rs-fMRI and 0.7762 ($P = .0221$) using pseudo-rs-fMRI for cognitive impairment status classification. The difference in AUC for pseudo-rs-fMRI and rs-fMRI was not statistically significant ($P = .29$). The asterisk indicates statistical significance.

95% CI, 0.7445–1.000; $P = .0013$; pseudo-rs-fMRI: AUC = 0.7762; 95% CI, 0.5892–0.9633; $P = .0221$, Fig 5), and there was no statistically significant difference between the 2 AUCs for classification ($P = .29$). There was also no significant relationship between tumor hemispheric lateralization and cognitive impairment status ($P > .99$).

DISCUSSION

A major barrier for the widespread use of clinical rs-fMRI outside of select institutions for presurgical planning[3-7] and functional mapping of patients with brain tumors is the additional time and cost requirements. Results from the current study suggest that pseudo-rs-fMRI derived from DSC perfusion MRI may be useful for performing network mapping, seed-to-voxel, and ROI-to-ROI resting-state analyses similar to rs-fMRI in patients with gliomas and cognitive assessment. The novelty and potential clinical utility of our method is that our pseudo-rs-fMRI approach using DSC perfusion MRI may theoretically preclude the need for an additional rs-fMRI scan because DSC perfusion MRI can provide combined advantages of assessing FC related to network mapping and cognition, while simultaneously providing perfusion estimates of tumor vascularity. The observation that alterations in rs-fMRI correspond with functional impairment is consistent with traditional rs-fMRI studies in developmental disorders,[33] aging,[34] and other neurologic diseases,[35,36] but the ability to estimate these rs-fMRI metrics quickly and concurrently with DSC perfusion MRI metrics within clinical workflows using the proposed DSC postprocessing technique opens up the possibility of estimating a wide range of rs-fMRI parameters in patients with brain tumors, including graph theory metrics,[10,12] within-tumor connectivity,[37] and BOLD asynchrony,[38] as well as broad applicability to other neurologic disorders that require evaluation of DSC perfusion, including stroke.

While our results suggested default mode, motor, and language network maps generated using pseudo-rs-fMRI derived from DSC perfusion were similar to maps using full rs-fMRI based on the Dice scores shown in the Online Supplemental Data, the pseudo-rs-fMRI-derived maps appeared noisier compared with rs-fMRI-derived maps at the patient-level, while the group-average network maps appeared more similar as quantified by the higher Dice scores for the group maps. This observation may be explained by the fact that DSC perfusion MRI is typically acquired for at least 2 minutes[39] (typically on the order of 2–3 minutes, ~3 minutes in the current study), while a traditional rs-fMRI is recommended to be acquired longer for at least 6 minutes (~10 minutes in the current study),[21,40] directly leading to increased noise in the estimation of connectivity from a decreased signal-to-noise ratio using pseudo-rs-fMRI. In support of this primary source of noise, truncating the full rs-fMRI to the first 100 timepoints (~3 minutes) resulted in similar Dice scores between pseudo-rs-fMRI and truncated rs-fMRI compared with the full rs-fMRI data set. However, there was variation in the Dice scores, and for the motor network, the Dice scores for pseudo-rs-fMRI were significantly higher than those of truncated rs-fMRI, perhaps due to variations in noise, so other factors beyond scan duration must be considered.

One additional source of this variation could be contributions to the DSC perfusion experiment itself, even after the contrast agent bolus is subtracted from the signal. It should be noted that even for rs-fMRI, even a slight variation in the patient's "rest" scanning condition such as simply whether patients keep their eyes open and fixated or keeps their eyes closed can impact the BOLD signal and the quality of rs-fMRI results.[40] Recent rs-fMRI guidelines for presurgical planning now even recommend eyes being kept open and fixated for the standardization of rs-fMRI.[21] However, in DSC perfusion MRI, patients are not instructed regarding eye fixation as it is not relevant for perfusion analyses, and there are additional sensory stimulations of the intravenous catheter and the delivery of contrast agent bolus during a DSC perfusion MRI that are not present during a typical rs-fMRI scan that may theoretically impact the resulting BOLD signal.

Another source of variation is likely related to differences in acquisition parameters between rs-fMRI and DSC perfusion MRI. Rs-fMRI scanning protocols are optimized to detect the BOLD signal, while DSC perfusion MRI protocols are optimized to quantify CBV and other perfusion metrics. Furthermore, the current study had variation in DSC perfusion MRI protocols, but some of these effects may have been mitigated through the use of leakage correction.[29,30] However, the methodology and results presented demonstrate the ability to generate FC network maps and identify patients with cognitive impairment despite these potential sources of contamination.

Of note, our proposed pseudo-rs-fMRI method involves postprocessing of DSC perfusion MRI that can be conducted retrospectively in institutional patient image databases, as done in the present study, as well as integrated into prospective image-acquisition workflows optimized for DSC perfusion MRI and pseudo-rs-fMRI analyses. Ideally, a DSC perfusion MRI protocol that is dually-optimized for pseudo-rs-fMRI and perfusion analyses in brain tumors may involve (i) increasing the scan acquisition to

6 minutes to be compliant with rs-fMRI guidelines[21] but (ii) within the suggested maximal 8-minute delay between contrast agent injection and 3D postcontrast T1-weighted MRI in the standardized Brain Tumor Imaging Protocol[41] and then (iii) cropping the signal to a shorter duration for perfusion analyses, to be compliant with DSC perfusion MRI guidelines.[39] Increasing the slice coverage of DSC perfusion MRI to consistently cover the entire brain, such as with simultaneous multislice techniques,[42] could allow further FC investigation of the uppermost superior regions such as the supplementary motor area[43] and lowermost inferior regions such as the cerebellum,[44] both of which were unable to be explored in the present ROI-to-ROI analyses using pseudo-rs-fMRI. It is also conceivable that the proposed pseudo-rs-fMRI method can be utilized with multiecho DSC perfusion MRI protocols for further flexibility in sequence parameters.[45]

It is important noting that the present study appeared to be underpowered, in that we consistently observed FWE-/FDR-uncorrected FC differences between cognitively impaired and nonimpaired patients using full rs-fMRI and pseudo-rs-fMRI, and no differences after traditional FWE-/FDR-correction. For example, without FWE-/FDR-correction, there were consistent FC difference patterns in the default mode network, notably a finding of increased connectivity between the medial prefrontal cortex and the rostral prefrontal cortex of the salience network in nonimpaired patients versus impaired patients as observed in a prior study[14] and increased connectivity between the medial prefrontal cortex and precuneus and posterior cingulate cortex of the default mode network in impaired versus nonimpaired patients. The latter finding of increased default mode network connectivity in impaired patients may reflect a compensatory mechanism that has been previously observed in patients with brain tumors[46] and mild cognitive impairment compared with healthy controls.[47] The slight differences in seed-to-voxel and ROI-to-ROI results may be due to the lost spatial specificity of small clusters when performing ROI-to-ROI analyses. While the present results should be interpreted with caution because of the lack of FWE-/FDR-correction and limited sample size, these findings demonstrate the potential of pseudo-rs-fMRI for FC group analyses using seed-to-voxel and ROI-to-ROI approaches that should be validated in studies with larger sample sizes, which may also resolve the slight differences in seed-to-voxel and ROI-to-ROI results and usage of empiric cluster thresholds. Nevertheless, the multiple logistic regression results utilizing a *combination* of FC measures demonstrate that our DSC perfusion MRI-derived pseudo-rs-fMRI approach may potentially have clinical utility in developing FC-based models for assessing a patient's cognitive status, and that these models would yield statistically similar results if rs-fMRI was acquired.

This study has some limitations that should be addressed. First, the sample size was limited. It should be recognized that the present study utilized a unique study cohort that underwent DSC perfusion MRI, rs-fMRI, and cognitive assessment because this cohort would be valuable for a first demonstration of the proposed pseudo-rs-fMRI approach. Future studies with increased sample size and a fully-balanced impaired-versus-nonimpaired distribution would be beneficial to validate the present study's observations and to longitudinally explore any associations of cognitive impairment with treatment. Additionally, although there are efforts in the standardization of DSC perfusion MRI protocols,[39] there remains much heterogeneity in DSC perfusion MRI protocols across institutions, which may impact the generalizability of our findings. A multicenter assessment of our proposed pseudo-rs-fMRI technique with various DSC perfusion MRI protocols (e.g., sequence parameters, imaging systems, contrast agent amount, preload) would be very valuable. Resting-state analyses have also been previously explored utilizing arterial spin-labeling (ASL) perfusion MRI,[48] which is an exogenous contrast agent-less perfusion MRI technique with T2*-weighting. However, some advantages of our proposed DSC-derived technique are that DSC perfusion MRI has higher spatial resolution and is more widely used in patients with gliomas than ASL perfusion MRI. Of course, DSC perfusion MRI involves a contrast agent bolus while ASL perfusion does not, similar to rs-fMRI, which is why we performed voxelwise bolus modeling after leakage-correction to generate pseudo-rs-fMRI data from DSC perfusion MRI to minimize the impact of contrast agent. Nevertheless, future studies may consider exploring other strategies to remove the contrast agent effect on the DSC perfusion MRI signal as well as comparing ASL perfusion MRI-derived and DSC perfusion MRI-derived rs-fMRI FC analyses. Lastly, a future study utilizing both pseudo-rs-fMRI and task-based fMRI may be interesting, as done similarly in a prior study using rs-fMRI and task-based fMRI for assessing language dominance.[3]

CONCLUSIONS
Pseudo-rs-fMRI data derived from DSC perfusion MRI can be used to perform typical rs-fMRI FC analyses that may identify cognitive decline in patients with brain tumors while still simultaneously performing perfusion analyses.

REFERENCES
1. Biswal B, Yetkin FZ, Haughton VM, et al. **Functional connectivity in the motor cortex of resting human brain using echo-planar MRI.** *Magn Reson Med* 1995;34:537–41 Medline
2. Pasquini L, Peck KK, Jenabi M, et al. **Functional MRI in neuro-oncology: state of the art and future directions.** *Radiology* 2023;308: e222028 CrossRef Medline
3. Gohel S, Laino ME, Rajeev-Kumar G, et al. **Resting-state functional connectivity of the middle frontal gyrus can predict language lateralization in patients with brain tumors.** *AJNR Am J Neuroradiol* 2019;40:319–25 CrossRef Medline
4. Kumar VA, Heiba IM, Prabhu SS, et al. **The role of resting-state functional MRI for clinical preoperative language mapping.** *Cancer Imaging* 2020;20:47 CrossRef Medline
5. Leuthardt EC, Guzman G, Bandt SK, et al. **Integration of resting state functional MRI into clinical practice: a large single institution experience.** *PLoS One* 2018;13:e0198349 CrossRef Medline
6. Sair HI, Yahyavi-Firouz-Abadi N, Calhoun VD, et al. **Presurgical brain mapping of the language network in patients with brain tumors using resting-state fMRI: comparison with task fMRI.** *Hum Brain Mapp* 2016;37:913–23 CrossRef Medline
7. Tie Y, Rigolo L, Norton IH, et al. **Defining language networks from resting-state fMRI for surgical planning: a feasibility study.** *Hum Brain Mapp* 2014;35:1018–30 CrossRef Medline

8. Greicius MD, Krasnow B, Reiss AL, et al. **Functional connectivity in the resting brain: a network analysis of the default mode hypothesis.** *Proc Natl Acad Sci U S A* 2003;100:253–58 CrossRef Medline

9. Greicius MD, Supekar K, Menon V, et al. **Resting-state functional connectivity reflects structural connectivity in the default mode network.** *Cereb Cortex* 2009;19:72–78 CrossRef Medline

10. Huang Q, Zhang R, Hu X, et al. **Disturbed small-world networks and neurocognitive function in frontal lobe low-grade glioma patients.** *PLoS One* 2014;9:e94095 CrossRef Medline

11. Kocher M, Jockwitz C, Caspers S, et al. **Role of the default mode resting-state network for cognitive functioning in malignant glioma patients following multimodal treatment.** *Neuroimage Clin* 2020;27:102287 CrossRef Medline

12. Noll KR, Chen HS, Wefel JS, et al. **Alterations in functional connectomics associated with neurocognitive changes following glioma resection.** *Neurosurgery* 2021;88:544–51 CrossRef Medline

13. Seitzman BA, Anandarajah H, Dworetsky A, et al. **Cognitive deficits and altered functional brain network organization in pediatric brain tumor patients.** *Brain Imaging Behav* 2023;17:689–701 CrossRef Medline

14. Wang C, Van Dyk K, Cho N, et al. **Characterization of cognitive function in survivors of diffuse gliomas using resting-state functional MRI (rs-fMRI).** *Brain Imaging Behav* 2022;16:239–51 CrossRef Medline

15. Nayak L, DeAngelis LM, Brandes AA, et al. **The Neurologic Assessment in Neuro-Oncology (NANO) scale: a tool to assess neurologic function for integration into the Response Assessment in Neuro-Oncology (RANO) criteria.** *Neuro Oncol* 2017;19:625–35 CrossRef Medline

16. Correa DD. **Neurocognitive function in brain tumors.** *Curr Neurol Neurosci Rep* 2010;10:232–39 CrossRef Medline

17. Kickingereder P, Sahm F, Radbruch A, et al. **IDH mutation status is associated with a distinct hypoxia/angiogenesis transcriptome signature which is non-invasively predictable with rCBV imaging in human glioma.** *Sci Rep* 2015;5:16238 CrossRef Medline

18. Leu K, Ott GA, Lai A, et al. **Perfusion and diffusion MRI signatures in histologic and genetic subtypes of WHO grade II–III diffuse gliomas.** *J Neurooncol* 2017;134:177–88 CrossRef Medline

19. Fatterpekar GM, Galheigo D, Narayana A, et al. **Treatment-related change versus tumor recurrence in high-grade gliomas: a diagnostic conundrum—use of dynamic susceptibility contrast-enhanced (DSC) perfusion MRI.** *AJR Am J Roentgenol* 2012;198:19–26 CrossRef Medline

20. Kim YH, Oh SW, Lim YJ, et al. **Differentiating radiation necrosis from tumor recurrence in high-grade gliomas: assessing the efficacy of 18F-FDG PET, 11C-methionine PET and perfusion MRI.** *Clin Neurol Neurosurg* 2010;112:758–65 CrossRef Medline

21. Kumar VA, Lee J, Liu HL, et al. **Recommended resting-state fMRI acquisition and preprocessing steps for preoperative mapping of language and motor and visual areas in adult and pediatric patients with brain tumors and epilepsy.** *AJNR Am J Neuroradiol* 2024;45:139–48 CrossRef Medline

22. Wefel JS, Vardy J, Ahles T, et al. **International Cognition and Cancer Task Force recommendations to harmonise studies of cognitive function in patients with cancer.** *Lancet Oncol* 2011;12:703–08 CrossRef Medline

23. Reijneveld JC, Sitskoorn MM, Klein M, et al. **Cognitive status and quality of life in patients with suspected versus proven low-grade gliomas.** *Neurology* 2001;56:618–23 CrossRef Medline

24. Ingraham LJ, Aiken CB. **An empirical approach to determining criteria for abnormality in test batteries with multiple measures.** *Neuropsychology* 1996;10:120–24 CrossRef

25. Ellingson BM, Bendszus M, Boxerman J, et al; Jumpstarting Brain Tumor Drug Development Coalition Imaging Standardization Steering Committee. **Consensus recommendations for a standardized Brain Tumor Imaging Protocol in clinical trials.** *Neuro Oncol* 2015;17:1188–98 CrossRef Medline

26. Whitfield-Gabrieli S, Nieto-Castanon A. **Conn: a functional connectivity toolbox for correlated and anticorrelated brain networks.** *Brain Connect* 2012;2:125–41 CrossRef Medline

27. Jenkinson M, Beckmann CF, Behrens TEJ, et al. **FSL.** *Neuroimage* 2012;62:782–90 CrossRef Medline

28. Otten ML, Mikell CB, Youngerman BE, et al. **Motor deficits correlate with resting state motor network connectivity in patients with brain tumours.** *Brain* 2012;135:1017–26 CrossRef Medline

29. Leu K, Boxerman JL, Cloughesy TF, et al. **Improved leakage correction for single-echo dynamic susceptibility contrast perfusion MRI estimates of relative cerebral blood volume in high-grade gliomas by accounting for bidirectional contrast agent exchange.** *AJNR Am J Neuroradiol* 2016;37:1440–46 CrossRef Medline

30. Leu K, Boxerman JL, Lai A, et al. **Bidirectional contrast agent leakage correction of dynamic susceptibility contrast (DSC)-MRI improves cerebral blood volume estimation and survival prediction in recurrent glioblastoma treated with bevacizumab.** *J Magn Reson Imaging* 2016;44:1229–37 CrossRef Medline

31. Cox RW. **AFNI: software for analysis and visualization of functional magnetic resonance neuroimages.** *Comput Biomed Res* 1996;29:162–73 CrossRef Medline

32. Hanley JA, McNeil BJ. **A method of comparing the areas under receiver operating characteristic curves derived from the same cases.** *Radiology* 1983;148:839–43 CrossRef Medline

33. Rudie JD, Brown JA, Beck-Pancer D, et al. **Altered functional and structural brain network organization in autism.** *Neuroimage Clin* 2012;2:79–94 CrossRef Medline

34. Tomasi D, Volkow ND. **Aging and functional brain networks.** *Mol Psychiatry* 2012;17:549–58 CrossRef Medline

35. Wang K, Liang M, Wang L, et al. **Altered functional connectivity in early Alzheimer's disease: A resting-state fMRI study.** *Hum Brain Mapp* 2007;28:967–78 CrossRef Medline

36. Park CH, Chang WH, Ohn SH, et al. **Longitudinal changes of resting-state functional connectivity during motor recovery after stroke.** *Stroke* 2011;42:1357–62 CrossRef Medline

37. Daniel AGS, Park KY, Roland JL, et al. **Functional connectivity within glioblastoma impacts overall survival.** *Neuro Oncol* 2021;23:412–21 CrossRef Medline

38. Petridis PD, Horenstein CI, Pereira B, et al. **BOLD asynchrony elucidates tumor burden in IDH-mutated gliomas.** *Neuro Oncol* 2022;24:78–87 CrossRef Medline

39. Boxerman JL, Quarles CC, Hu LS, et al; Jumpstarting Brain Tumor Drug Development Coalition Imaging Standardization Steering Committee. **Consensus recommendations for a dynamic susceptibility contrast MRI protocol for use in high-grade gliomas.** *Neuro Oncol* 2020;22:1262–75 CrossRef Medline

40. Van Dijk KR, Hedden T, Venkataraman A, et al. **Intrinsic functional connectivity as a tool for human connectomics: theory, properties, and optimization.** *J Neurophysiol* 2010;103:297–321 CrossRef Medline

41. Ellingson BM, Bendszus M, Boxerman J, et al; Jumpstarting Brain Tumor Drug Development Coalition Imaging Standardization Steering Committee. **Consensus recommendations for a standardized brain tumor imaging protocol in clinical trials.** *Neuro Oncol* 2015;17:1188–98 CrossRef Medline

42. Chakhoyan A, Leu K, Pope WB, et al. **Improved spatiotemporal resolution of dynamic susceptibility contrast perfusion MRI in brain tumors using simultaneous multi-slice echo-planar imaging.** *AJNR Am J Neuroradiol* 2018;39:43–45 CrossRef Medline

43. Bathla G, Gene MN, Peck KK, et al. **Resting state functional connectivity of the supplementary motor area to motor and language networks in patients with brain tumors.** *J Neuroimaging* 2019;29:521–26 CrossRef Medline

44. Cho NS, Peck KK, Gene MN, et al. **Resting-state functional MRI language network connectivity differences in patients with brain tumors: exploration of the cerebellum and contralesional hemisphere.** *Brain Imaging Behav* 2022;16:252–62 CrossRef Medline

45. Stokes AM, Bergamino M, Alhilali L, et al. **Evaluation of single bolus, dual-echo dynamic susceptibility contrast MRI protocols in brain tumor patients.** *J Cereb Blood Flow Metab* 2021;41:3378–90 CrossRef Medline

46. Tordjman M, Madelin G, Gupta PK, et al. **Functional connectivity of the default mode, dorsal attention and fronto-parietal executive control networks in glial tumor patients.** *J Neurooncol* 2021;152:347–55. CrossRef Medline

47. Gardini S, Venneri A, Sambataro F, et al. **Increased functional connectivity in the default mode network in mild cognitive impairment: a maladaptive compensatory mechanism associated with poor semantic memory performance.** *J Alzheimers Dis* 2015;45:457–70 CrossRef Medline

48. Zhu S, Fang Z, Hu S, et al. **Resting-state brain function analysis using concurrent BOLD in ASL perfusion fMRI.** *PL0S One* 2013;8: e65884 CrossRef Medline